Pulse Sharpening and Gain Saturation in Traveling-Wave Masers*

By E. O. SCHULZ-DuBOIS

(Manuscript received September 12, 1963)

A pair of coupled nonlinear differential equations is given which describes the reduction of gain in a traveling-wave maser due to high-power signals. Integrals in closed form are obtained for two cases of interest. The first applies to pulsed optical amplifiers where no replacement of stored energy occurs during a signal pulse. The result is a pulse sharpening phenomenon; i.e., the leading edge of an input pulse is amplified by the original full gain while later parts of the signal experience reduced gain. The second case is that of steady-state gain saturation in the presence of a continuous pumping process. The results describe the observed gain compression of microwave ruby traveling-wave masers.

1. INTRODUCTION

This paper presents earlier considerations concerning the gain process in traveling-wave masers in cases where the signal energy, over an appropriate period of time, is comparable to the energy stored in the maser material. The results were communicated several years ago in reports with limited circulation.[1,2,3] The studies were prompted originally by the development of microwave masers, in particular the ruby comb-structure traveling-wave maser.[4] Here gain saturation is of interest primarily in a negative sense: it is a condition that should be avoided in system applications. The maser may handle input signals up to some typical saturation limit which depends on the tolerable gain compression, the signal duty ratio, and the low-power gain. Thus the situation of drastic gain reduction due to saturation is largely of academic interest. It may be used, however, as a check on the theoretical understanding of the maser gain process.[3] It should be added that even with drastically compressed gain the maser is still a linear amplifier in the sense that it does

* This work was supported in part by the U.S. Army Signal Corps under contracts No. DA 36-039 SC-73224 and SC-85357.

not create intermodulation frequencies due to a nonlinear mixing interaction. Rather, the output is still a faithfully scaled replica of the input signal.[5,6]

The advent of optical masers in more recent years[7,8,9] has led to a more genuine interest in maser high-power saturation phenomena. The generation of high-power ("giant") pulses by the Q-switching technique,[10] for example, makes use of the fast exhaustion of the energy stored in the maser material. Similarly, pulse sharpening is an inevitable and in some applications a desirable effect in a pulsed high-power postamplifier.[11,12] The more prominent role of high-power phenomena in the optical maser field has suggested the present, more complete publication of the earlier reports.

The theory of masers is largely identical for those in the microwave and in the optical range. This applies, for example, to the derivations of the gain and noise behavior. The same is true for the high-power phenomena treated in the present paper. Thus the term traveling-wave maser (TWM) can be used without further distinction except in numerical examples.

The coupled differential equations governing the TWM high-power behavior are given in the following section. The integral applicable to pulsed TWM's is derived in Section III. Some numerical consequences for pulse sharpening are discussed in Section IV, and an experimental example of pulsed optical TWM performance is analyzed in Section V. The integrals describing steady-state gain saturation are derived, and computed gain saturation curves are presented, in Section VI. Experimental gain saturation data obtained with a microwave TWM are shown for comparison in Section VII.

II. THE DIFFERENTIAL EQUATIONS

The gain process in the TWM is stimulated emission. It is the interaction of two forms of energy. One is the radiation energy of the mode under consideration. Its strength may be measured in terms of the number of photons per unit of time, $n_t'(z',t')$, which pass the maser or the mode cross-section at a point z' along the maser length and at a time t'. Here z' ranges from $z' = 0$ at the input to $z' = L$ at the output. In the absence of gain or loss interaction, the radiation energy propagates through the maser with a group velocity v_g, so that then $n_t' \equiv n_t'(z' - v_g t')$.

The other form of energy is that stored in the maser material. It can be given in terms of the number of available quanta per unit of maser

length, $n_z'(z',t')$, within the cross section occupied by the signal transmission mode. The number of available quanta is half the excess number of particles in the upper state of the signal transition over those in the lower state, $n_z' = \frac{1}{2}(n_2' - n_1')$. n_z' may depend on the length coordinate z' along the TWM and on time t'. A quantity N_z may be introduced as the "pumped-up value" of n_z'. It is the maximum value which n_z' may assume either with low signal power operation under steady-state conditions or before any signal energy withdrawal with pulsed pump operation.

Using these energy variables, a system of two coupled partial differential equations may be given which describes the high-power effects in TWMs. It is of first order and nonlinear

$$\frac{\partial n_t'}{\partial z'} + \frac{1}{v_g}\frac{\partial n_t'}{\partial t'} = a n_t' n_z' - b n_t' \tag{1}$$

$$\frac{\partial n_z'}{\partial t'} = -a n_t' n_z' + c(N_z - n_z'). \tag{2}$$

The first terms on the right-hand side are equal and opposite. This is an expression of energy conservation; i.e., each quantum of energy stored in the maser material is converted into a photon propagating in the signal mode. In a maser, energy conservation of this type may be a justified assumption, at least under high-power conditions where other processes such as spontaneous transitions are insignificant by comparison.

The dimensionless constant a describes the gain interaction between both forms of energy. In units of decibels, the low-power electronic gain of the TWM is $4.35\ a\ N_z L$. This allows a numerical evaluation of the constant a from experimental data. The line shape of the maser transition is reflected in the frequency dependence of a. Implicit in such a treatment of line shape is the assumption that the maser transition considered is homogeneously broadened. However, the present theory may also be applied to lines with inhomogeneous broadening provided the energy diffusion across the overall line is rapid enough to prevent a line shape distortion or "hole burning" under high-power conditions. Formally, for a magnetic dipole transition at the maser signal line, a can be given in the form

$$a = \frac{2\pi\omega g(\nu - \nu_{nn'}) \int_{A_M} | < n' | g\beta \bar{H}\cdot\bar{S} | n > |^2 \, dA}{v_g h \mu_0 A_M \int_{A_S} | H |^2 \, dA}. \tag{3a}$$

Here $\omega/2\pi = \nu$ = signal frequency, $g(\nu - \nu_{nn'})$ = line shape function, $\langle n' \mid g\beta\bar{H}\cdot\bar{S} \mid n\rangle$ = matrix element of the transition, v_g = group velocity, h = Planck's constant, μ_0 = vacuum permeability, A_M = cross section of maser material, A_S = cross section of structure; finally, the ratio of the magnetic field energy integrals alone in (3a) defines the filling factor. The symbols used are those introduced in Ref. 4, to which the reader is referred for a derivation of traveling-wave maser theory. In the optical range it is more convenient to characterize a maser line by its spontaneous transition rate, $W(\theta,\varphi,\bar{P})$, which is a function of the direction of emission expressed by spherical angular coordinates θ and φ, and of the polarization $\bar{P}$ of the emitted light. Using this term, a becomes

$$a = \frac{2\lambda_0^2 g(\nu - \nu_0) W(\theta,\varphi,\bar{P})}{\epsilon A_m} \tag{3b}$$

where λ_0 = vacuum wavelength of light, $g(\nu - \nu_0)$ = line shape function, ϵ = dielectric constant of maser material, A_m = cross section of amplified mode. These symbols are defined as in Ref. 11, where the theory of optical traveling-wave maser amplifiers is derived.

The constant b accounts for signal loss along the TWM. In a microwave TWM it may consist of ohmic structure losses (copper loss) and the forward attenuation of the isolator (ferrite loss). In an optical TWM, the losses may be contributed by scattering, diffraction and the isolator, although the latter two do not really occur in a distributed fashion. In units of decibels, the total propagation loss in the maser is 4.35 bL.

For the case of CW pumping, a maser recovery rate c is included in (2). It is the reciprocal of the exponential time constant which describes the low-power gain recovery after a saturating pulse. In microwave masers the pump power usually available is relatively high, so that c is essentially given by the spin-lattice relaxation rate of the idler transition. In CW optical masers the pump levels usually available tend to be lower in terms of pump photons, so that c may be largely determined by the pump power.

The left-hand side of (1) is a combination of partial derivatives with respect to time t' and space z', which indicates that signal propagation with a group velocity v_g is considered in the positive z' direction. Propagation in the negative z' direction would require a minus sign. The complication of propagation effects can be eliminated from (1) by a transformation

$$\begin{aligned} z &= z' & \qquad n_t' &= n_t \\ v_g t &= v_g t' - z' & \qquad n_z' &= n_z \end{aligned} \tag{4}$$

which results in the differential equations

$$\frac{\partial n_t}{\partial z} = an_t n_z - bn_t \tag{5}$$

$$\frac{\partial n}{\partial t} = -an_t n_z + c(N_z - n_z). \tag{6}$$

The physical situation and this transformation in particular are illustrated in the space-time diagram of Fig. 1. It is seen that the new time coordinate t remains constant for any part of the signal as it passes from the input to the output. For example, the leading edge of a pulse is char-

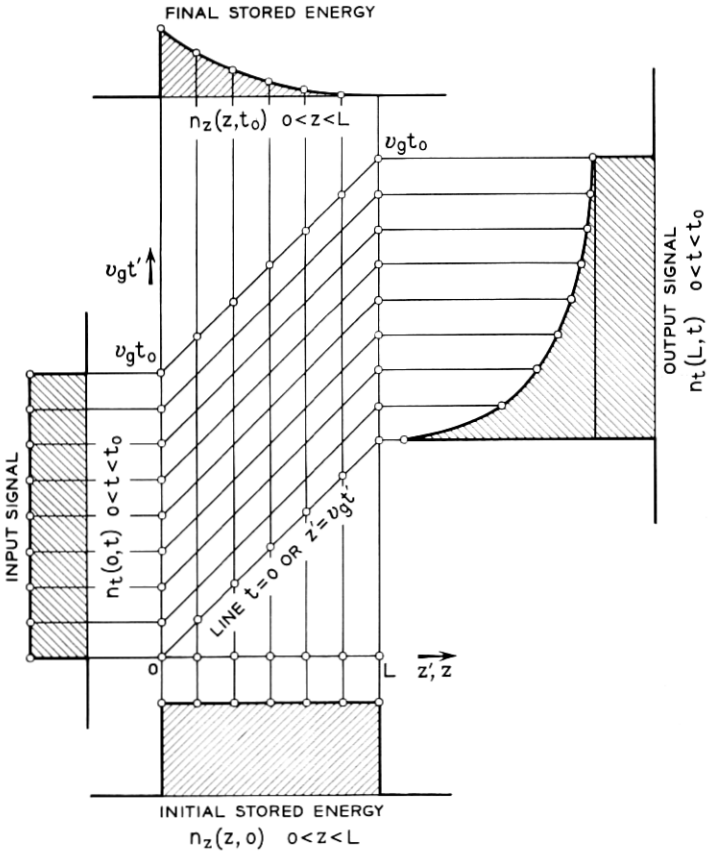

Fig. 1 — Schematic presentation of the maser gain process by removal of stored energy; also shown are space and time coordinate systems.

acterized by $t = 0$, whereas in real time it would pass the input at $t' = 0$ and the output at $t' = L/v_g$.

The figure also suggests that the problem contained in (5) and (6) is hyperbolic in nature; that is, it is characteristic of propagation. In the present case this implies that the physical situation at a point z,t is determined by all interactions which happened earlier, i.e., from time 0 to t, and closer, i.e., from 0 to z. Such a problem is not specified unless two boundary conditions are set up. The first is an initial condition which specifies the situation for values of z, $0 < z < L$, at the time $t = 0$. The second is an input condition which specifies the situation for times t, $t > 0$, at the input $z = 0$. Then the equations permit a unique evaluation of the variables at any point z and time t.

The boundary conditions for the present problem include the initial stored energy

$$n_z(z,t = 0) = \begin{cases} n_z(z) & \text{for } 0 < z < L \\ 0 & \text{for } z < 0 \text{ and } L < z \end{cases} \tag{7a}$$

and in the simplest case may involve a uniform distribution of stored energy

$$n_z(z,t = 0) = \begin{cases} N_z & \text{for } 0 < z < L \\ 0 & \text{for } z < 0 \text{ and } L < z. \end{cases} \tag{7b}$$

The other condition specifies the input signal

$$n_t(z = 0,t) = \begin{cases} n_t(t) & \text{for } t > 0 \\ 0 & \text{for } 0 > t \end{cases} \tag{8a}$$

which in the simplest case may consist of a step function signal

$$n_t(z = 0,t) = \begin{cases} N_t & \text{for } t > 0 \\ 0 & \text{for } 0 > t. \end{cases} \tag{8b}$$

It turns out that the equation system (5) and (6) with the boundary conditions (7) and (8) cannot be integrated in general. An exact integral can be obtained, however, for $b = c = 0$. It will be derived in the next section. This integral describes the response of a maser amplifier with negligibly small internal losses and no replacement mechanism for the drain of stored energy. It is of interest, since these mathematical conditions approximate very closely the physical situation of pulsed solid-state optical maser amplifiers.

Another integral can be readily obtained from (5) and (6) by letting

$\partial n_z/\partial t = 0$ in (6) and with $b \neq 0$ and $c \neq 0$. This leads to the steady-state gain saturation formulas which are discussed in the later parts of this paper and which are of interest in applications of microwave TWMs.

For numerical calculations it may not be too convenient to interpret n_t as the number of photons per unit time and n_z as the number of stored quanta per unit length. Instead n_z may be made to mean the stored energy in joules per unit of maser length and n_t the signal power in joules per second, i.e. watts. This new convention changes the definition of the constant a in (3). Now 4.35 a becomes equal to the decibel electronic gain of a TWM under consideration divided by the energy stored (in units of joules) in the same TWM.

III. SOLUTION FOR THE TRANSIENT CASE

For $b = c = 0$, (5) and (6) can be conveniently rewritten

$$\frac{\partial n_t}{\partial z} + \frac{\partial n_z}{\partial t} = 0 \tag{9}$$

$$-a \frac{\partial n_z}{\partial t} = a^2 n_t n_z . \tag{10}$$

In this form, (9) is recognized as a conservation law. Using the language of gas kinetic chemical reactions, (10) describes a bimolecular reaction whose yield is proportional to the density of either molecular species, the photons and stored quanta in this case.

The integration of the system (9), (10) subject to the boundary conditions (7a) and (8a) is outlined in the following paragraphs of this section. The method of integration was suggested to the author by J. A. Morrison. It is presented here because it does not follow an established standard approach.

A new function Φ is introduced subject to the requirements

$$\frac{\partial \Phi}{\partial z} = -an_z , \qquad \frac{\partial \Phi}{\partial t} = an_t . \tag{11}$$

This "ansatz" satisfies (9) by definition, and the remaining differential equation (10) becomes

$$\frac{\dfrac{\partial}{\partial t}\dfrac{\partial \Phi}{\partial z}}{\dfrac{\partial \Phi}{\partial z}} = -\frac{\partial \Phi}{dt} . \tag{12}$$

Logarithmic integration with respect to t yields

$$\ln \frac{d\Phi}{dz} = -\Phi + \ln \frac{dF(z)}{dz} \tag{13}$$

where the last term is an integration constant which may be a function of z alone. After rearrangement this is

$$e^{\Phi} \frac{\partial \Phi}{\partial z} = \frac{dF(z)}{dz}. \tag{14}$$

A second integration is possible, with the result

$$e^{\Phi} = F(z) + K(t) \tag{15}$$

or

$$\Phi = \ln [F(z) + K(t)] \tag{16}$$

where K is an arbitrary function of t alone.

The as yet arbitrary functions F and K are specified by the boundary conditions (7a) and (8a). Using these and the definition of Φ in (11), one has

$$n_t(t) = \frac{1}{a} \frac{d\Phi(z = 0)}{dt} = \frac{1}{a} \frac{\dfrac{dK(t)}{dt}}{F(0) + K(t)} \qquad \text{for } t < 0 \tag{17}$$

$$n_z(z) = -\frac{1}{a} \frac{d\Phi(t = 0)}{dz} = -\frac{1}{a} \frac{\dfrac{dF(z)}{dz}}{F(z) + K(0)} \qquad \text{for } 0 < z < L. \tag{18}$$

These equations can be easily integrated and the results may be combined in the form

$$\exp\left[a \int_0^t n_t(s)\,ds\right] + \exp\left[-a \int_0^z n_z(u)\,du\right] - 1 = \frac{F(z) + K(t)}{F(0) + K(0)}. \tag{19}$$

When this result is inserted into (16) and the original definition of Φ, (11), the final solution is

$$n_t(z,t) = \frac{n_t(t)\quad S(t)^{-1}}{S(t)^{-1} + G(z)^{-1} - 1} \tag{20}$$

$$n_z(z,t) = \frac{n_z(z)\quad G(z)^{-1}}{S(t)^{-1} + G(z)^{-1} - 1} \tag{21}$$

where $G(z)$ is the initial power gain

$$G(z) = \exp\left[a \int_0^z n_z(u)\, du\right] \tag{22}$$

and $S(t)$ is the saturation parameter at the input, i.e., the fraction to which the original stored energy near the input is reduced after a time t

$$S(t) = \exp\left[-a \int_0^t n_t(s)\, ds\right]. \tag{23}$$

For the simpler boundary conditions (7b) of an initially uniform gain distribution and (8b) of a step function input signal, the solutions (20) and (21) take the form

$$n_t(z,t) = \frac{N_t \exp(aN_t t)}{\exp(aN_t t) + \exp(-aN_z z) - 1} \tag{24}$$

$$n_z(z,t) = \frac{N_z \exp(-aN_z z)}{\exp(aN_t t) + \exp(-aN_z z) - 1}. \tag{25}$$

The solutions (20) and (21) show a number of mathematical properties which should be expected in view of the physical situation. With general definitions for the gain and saturation parameters

$$\begin{aligned} G(z,t) &= n_t(z,t)/n_t(t) \\ S(z,t) &= n_z(z,t)/n_z(z) \end{aligned} \tag{26}$$

the following features may be mentioned:

(*i*) The gain $G(z,t)$ decreases monotonically with time from the initial value (22) down to unity. $G(z,t)$ is greater for larger values of z.

(*ii*) Similarly, the saturation parameter $S(z,t)$ decreases monotonically with time from the initial value of unity to zero. The drop is faster for greater values of z.

(*iii*) $G(z,t)$ may be expressed in the form (20) using the initial gain, but it may be also obtained by computing the gain due to the instantaneous excess energy storage $n_z(z,t)$. Thus

$$G(z,t) = \frac{S(t)^{-1}}{S(t)^{-1} + G(z)^{-1} - 1} = \exp\left[a \int_0^z n_z(u,t)\, du\right]. \tag{27}$$

(*iv*) A corresponding relation holds for $S(z,t)$

$$S(z,t) = \frac{G(z)^{-1}}{S(t)^{-1} + G(z)^{-1} - 1} = \exp\left[-a \int_0^t n_t(z,s)\, ds\right]. \tag{28}$$

(*v*) Fig. 1 suggests that the situation at some time t_1 might be used as

a boundary condition instead of the initial condition at time $t = 0$. Thus there is an addition theorem for the gain formula

$$\begin{aligned} G(z,t_1 + t_2) &= \frac{S(t_1 + t_2)^{-1}}{S(t_1 + t_2)^{-1} + G(z)^{-1} - 1} \\ &= \frac{S(t_2)^{-1}}{S(t_2)^{-1} + G(z,t_1)^{-1} - 1}. \end{aligned} \tag{29}$$

(*vi*) A similar iteration formula applies to the saturation parameter, which may be defined either directly by the initial total gain and input saturation or by the initial gain of a part of the maser and the saturation at the beginning of this part

$$\begin{aligned} S(z_1 + z_2,t) &= \frac{G(z_1 + z_2)^{-1}}{S(t)^{-1} + G(z_1 + z_2)^{-1} - 1} \\ &= \frac{G(z_2)^{-1}}{S(z_1,t)^{-1} + G(z_2)^{-1} - 1}. \end{aligned} \tag{30}$$

(*vii*) Energy conservation requires that the excess of the output energy over the input energy equal the loss in stored energy

$$\int_0^t [n_t(z,s) - n_t(s)]\, ds = \int_0^z [n_z(u) - n_z(u,t)]\, du. \tag{31}$$

Equations (27) to (31) may be verified directly.

Equations (20) to (21) can be simplified if the original gain is large, $G(z) \gg 1$, and if the degree of saturation at the input is small,

$$a \int_0^t n_t(s)\, ds \ll 1.$$

The greater part of the decrease in gain occurs before this last condition is violated. With these approximations

$$\frac{n_t(z,t)}{n_t(t)G(z)} = \frac{1}{1 + G(z)a \int_0^t n_t(s)\, ds} \tag{32}$$

$$\frac{n_z(z,t)}{n_z(z)} = \frac{1}{1 + G(z)a \int_0^t n_t(s)\, ds}. \tag{33}$$

Equations (32) and (33) describe a hyperbola, as shown in Fig. 2. In the case of a step function input signal (8b), for example, the curve describes directly the shape of the output signal. The initial output power

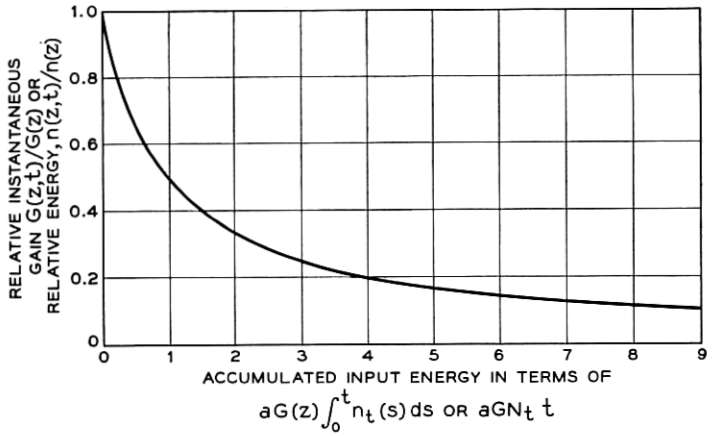

Fig. 2 — Decrease of gain as a function of input energy and decrease of stored energy vs input energy. The graph can be also interpreted as showing the shape of the output signal vs time if a step function input signal is applied.

in that case, of course, is given by the input signal multiplied by the original gain and the ordinate of the curve would have to be scaled accordingly. As one expects from energy conservation, the reciprocal scaling applies to the time scale on the abscissa. In other words, the drop of the output signal occurs faster if the input signal and the initial gain are higher. Also, as expected, the drop of the output sets in more slowly if the stored energy per db of initial gain, $(4.35\ a)^{-1}$, is greater.

The curve in Fig. 2 also describes the reduction of stored energy as a function of input energy. Directly at the input, the stored energy decays by an exponential law (23). Further along the TWM at points z, where there is an appreciable initial gain $G(z)$, the reduction of stored energy follows the hyperbolic law. The initial drop is faster for higher $G(z)$, but then the loss of stored energy levels off, although it is always faster than directly at the input.

The reduction of gain with input energy is plotted in another way in Fig. 3. Roughly speaking, the plot is a double logarithmic presentation of the data in Fig. 2. The ordinate shows the gain in db. The abscissa shows the decibel degree of saturation at the input

$$10 \log_{10} S(t) = 4.35\ a \int_0^t n(s)\ ds$$

plotted on a logarithmic scale. In this presentation, the hyperbola of Fig. 2 becomes a horizontal line curving into another line with a slope

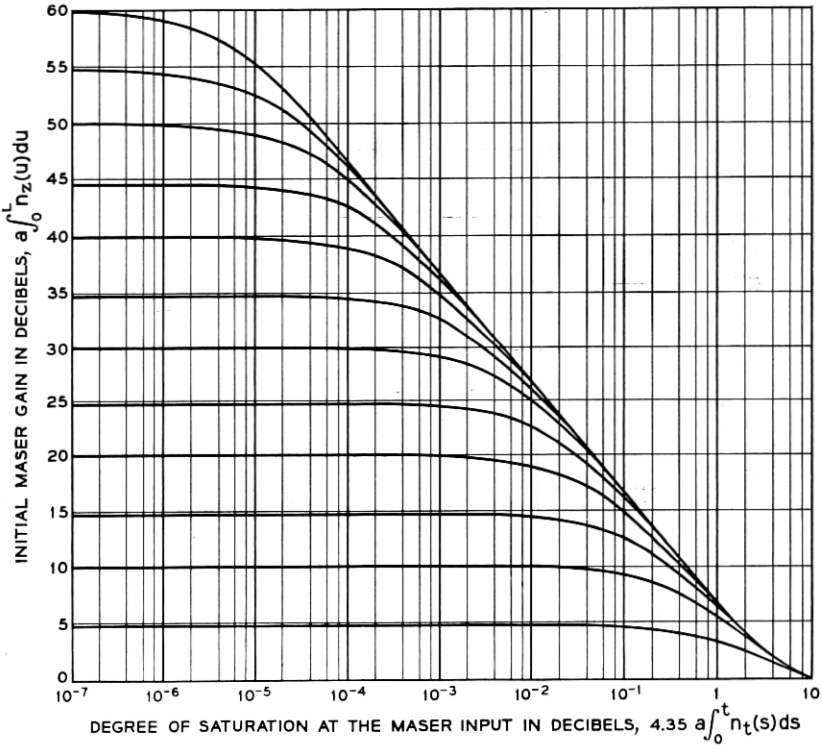

Fig. 3 — Drop of the initial gain in db vs integrated input energy, in db of saturation at the maser input. The plot shows that with the same constant input signal, the gain of a maser with initial 10 db higher gain drops 10 times faster.

of minus unity. A family of curves results because abscissa and ordinate now contain the initial gain explicitly. In this way the plot demonstrates that, of two otherwise identical TWMs excited by the same input signal, the one with a 10-db higher gain, for example, suffers gain reduction 10 times faster. In the lower right-hand of the figure it is seen that the asymptote to all curves is no longer a straight line but levels off. This is the region where the gain is very large compared to unity and the degree of saturation at the input is small. Thus there the expression (32) no longer approximates the gain behavior, and hence the exact formula (20) had to be used for plotting the curve.

IV. DISCUSSION OF PULSE SHARPENING

The results of the last section show that the instantaneous gain of a TWM is a decreasing function of time. The decrease can be particularly

rapid if the energy stored in the TWM is not too high. The question arises whether this phenomenon can be used as an optical pulse shaping mechanism. From a practical viewpoint, such a method of pulse generation would be of interest only if it could be used to produce pulses of higher peak power within a diffraction-limited beamwidth and/or of shorter duration than those produced by other methods. High peak power allows the study of nonlinear interactions in matter, and short pulses can be used in optical ranging devices with extremely high resolution. The generation of very short, very high-powered pulses will be discussed in this section with the aid of some numerical examples. These examples are deliberately chosen to be between the present state of the art and optimistic forecasts.

As a first example consider a step function input at a power of $N_t = 10^6$ watts incident on a unidirectional optical TWM of the type developed by Geusic and Scovil,[11] but with an initial gain of 40 db. The leading edge of the pulse experiences the initial gain and hence results in 10^{10} watts = 10 gigawatts at the output. The duration of the pulse may be defined as the time at which the output has dropped 3 db. It can be obtained from Fig. 2 or 3.

In the ruby optical TWM,[11] the stored energy is about 1 joule for every 6 db of gain, provided the signal transmission mode matches the cross section of the ruby rods. Thus $4.35\ a = 6$ db/joule. The gain is reduced 3 db after a time

$$t_{\frac{1}{2}} = (GaN_t)^{-1}. \tag{34}$$

For the numbers chosen, $t_{\frac{1}{2}} = 0.7 \times 10^{-10}$ seconds. The energy $\Delta E_{\frac{1}{2}}$ released by the TWM up to that time can be found, for example, by integrating (24) with respect to time. It can also be given without calculation, however, if one considers that at any time there is proportionality between the stored energy and the decibel gain. Thus $\Delta E_{\frac{1}{2}}$ is equal to the energy stored originally in a fraction of the amplifier length which initially gives rise to 3 db of gain:

$$\Delta E_{\frac{1}{2}} = \frac{3}{G_0(\text{db})} N_z L, \tag{35}$$

which is $\frac{1}{2}$ joule in the case considered.

With less stored energy in the amplifier, for example by signal transmission which utilizes only a fraction of the ruby cross section, the pulse duration $t_{\frac{1}{2}}$ would tend to be shorter. This is hardly possible, however, because the time given already comes close to the linewidth-limited rise time of the amplifier.

The computed pulse duration and peak power would seem rather attractive, and certainly they are beyond the capabilities of existing technology. It should be questioned whether the calculation is based on realistic assumptions. Geusic has operated a TWM with initial gain values of 20 to 30 db. Thus the assumed initial gain of 40 db is feasible. An optical power level in the megawatt range can be produced over short periods of time by the Q-switching technique.[10] Usually, however, that power is spread over a larger beam divergence than the diffraction minimum. Only a diffraction-limited beam can be fed conveniently into an aperture-limited TWM. The greatest discrepancy exists, however, with respect to the rise time of the input pulse, or step function, as used in the calculation. The calculation presented and the results are meaningful only if the input power rises in a time short compared to $t_{\frac{1}{2}}$ or at least comparable to it. If this were the case, the pulse would have its original fast rise and the exhaustion of the gain mechanism discussed here would produce a reasonably sharp cutoff at the trailing edge. Realistic rise times for Q-switched giant pulses are about two orders of magnitude longer than the $t_{\frac{1}{2}}$ quoted. With such a pulse fed into a TWM, most of the stored energy and amplification would be depleted long before the input ever reached the assumed 1 megawatt level.

The question therefore arises as to what degree of pulse forming may be observed under conditions when the input signal is a rising function of time. The situation is schematically indicated in Fig. 4. The input signal may be the initial rise of a giant pulse. A TWM with initial gain G_1 will amplify the first portion of the input signal proportionally until a noticeable fraction of the stored energy is exhausted. The resulting drop of gain may be so rapid that a distinguishable pulse is obtained at the output. With higher initial gain $G_2 > G_1$ in the amplifier, the peak power of the pulse is greater, the peak is reached sooner and the subsequent drop to $\frac{1}{2}$ of the peak power occurs faster.

The rise of the input signal may be described by a power law

$$n_t(t) = (t/t_0)^n P, \qquad n = 1, 2, 3 \cdots . \tag{36}$$

The numbers used in the example are a peak input power of $P = 10^6$ watt which is reached after a rise time of $t_0 = 10^{-8}$ second. The initial TWM gain considered is 60 db, $G(L) = 10^6$. Application of (32) shows that the peak of the output pulse occurs at a time $t_{\max}$ where

$$(t_{\max})^{n+1} = \frac{n(n+1)t_0{}^n}{aPG(L)} . \tag{37}$$

The output power is down 3 db from the peak value at the time $t_{\frac{1}{2}}$ where

$$t_{\frac{1}{2}} \approx 2\,\frac{n+1}{n}\,t_{\max}\,. \tag{38}$$

At the peak of the pulse the remaining gain is

$$G(L,t_{\max}) = \frac{1}{n+1}\,G(L) \tag{39}$$

and the peak output power $n_t(L,t_{\max})$ becomes

$$[n_t(L,t_{\max})]^{n+1} = \frac{PG(L)}{n+1}\left(\frac{n}{at_0}\right)^n. \tag{40}$$

Table I summarizes the numerical results. The true rise of the giant pulse may come sufficiently close to a cubic or quartic parabola. From the last two entries in the table one then can estimate that the peak of the output pulse will exceed the peak of the input by about 30 db. This is a sizable

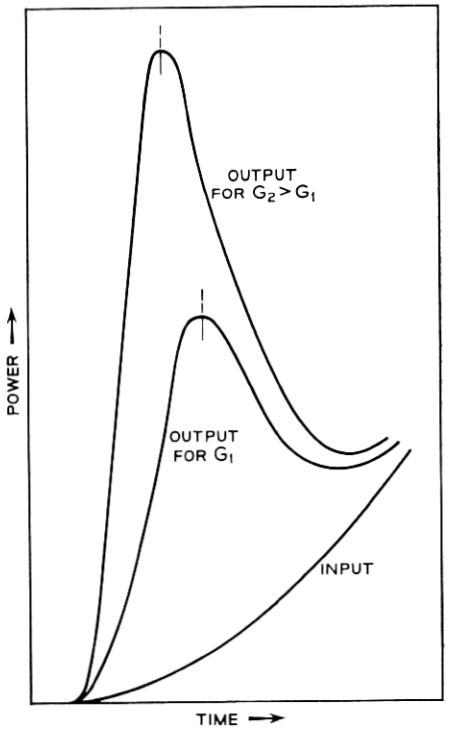

Fig. 4 — Pulse sharpening during rise time of input signal. The pulse is higher and the rise time shorter for higher initial gain.

TABLE I

Exponent of Input Rise [n in (36)]	Pulse Duration [$t_{\frac{1}{2}}$ in (38)]	Peak Pulse Power (watts) [$n_t(L,t_{max})$ in (40)]
$n = 1$ Straight-line rise	4.8×10^{-10} sec	6×10^{9}
$n = 2$ Quadratic parabola	2.3×10^{-9} sec	1.9×10^{9}
$n = 3$ Cubic parabola	4.6×10^{-9} sec	1.3×10^{9}
$n = 4$ Quartic parabola	6.7×10^{-9} sec	1.1×10^{9}

Values used: input: rise time $t_0 = 10^{-8}$ sec
maximum power $P = 10^{6}$ watt
maser: initial gain $G(L) = 10^{6}$
energy storage $(4.35\ a)^{-1} = 6$ db/joule

increase, although it is much less than the initial gain of 60 db. The pulse power obtained in this fashion from the TWM has essentially the same frequency spectrum and mode distribution as the input pulse. This can be understood by observing that the TWM is, for any short time element, a truly linear amplifier although the gain decreases continually with time. It is therefore clear that the output frequency spectrum is only slightly wider than that of the input, namely to the extent that the pulse duration was indeed shortened. Similarly, appreciable mode conversion by a TWM amplifier is possible only if the gain over the cross section is grossly nonuniform. In this sense, the TWM is a "faithful" amplifier even under high power saturating conditions. The duration of the pulse, measured here from $t = 0$ to the time $t_{\frac{1}{2}}$ when the output power has passed the peak value and dropped to $\frac{1}{2}$ of it, is at best not quite one order of magnitude shorter than the assumed initial build-up time t_0 of the input signal.

It is beyond the scope of this paper to suggest whether or not the pulse sharpening discussed is a practical way of producing the extreme in fast, high-power pulses. It is a way, however, where, although with diminishing returns, the peak power is only limited by whatever high-power limits exist in the stimulated emission process itself and in transmission through materials like glass and sapphire, and where the ultimate pulse rise time is limited only by the bandwidth of the maser signal line itself, not by the time for a round trip of light through the device, as in the Q-switched oscillator.

There remains one point which is more curious than serious. The reader might ask why the power law (36) was used for the input power in the pulse sharpening analysis. If instantaneous switching of the shutter can

be assumed, the initial rise of the giant pulse follows an exponential[13]

$$n_i(t) = P \exp (t/t_0) \qquad -t_1 < t < 0. \tag{41}$$

Is it possible to use this input signal for pulse sharpening analysis?

It turns out that the ideal exponential rise, $-t_1 = -\infty$, does not produce an output pulse at all. Rather, the output becomes a monotonically increasing function of time. Loosely speaking, the exponential input clears the stored energy out of the TWM in such a smooth fashion, slowly at first while the gain is still high and more rapidly when the gain has started to decrease, that it never can develop the kind of "overswing" or "shock wave" indicated in Fig. 4. One consequence is therefore that deviations from the exponential rise in the actual input signal are significant and helpful for achieving pulse sharpening.

V. AN EXPERIMENTAL EXAMPLE OF PULSE SHARPENING

One of the aims of optical traveling-wave maser development is the generation of very high pulse power by amplification of an already high input signal. Pulse sharpening due to partial exhaustion of the maser energy storage is unavoidable in this situation, as pointed out in the paper on the optical traveling-wave maser.[11] Even with more moderate power levels, some pulse sharpening can be observed if pulse duration and initial gain are sufficiently large. Geusic and Scovil[12] demonstrated the effect in experiments with the optical TWM, and an example of their observations is given in Fig. 5. It shows the tracing of a dual-beam oscilloscope presentation of pulse amplification. Part of the amplifier input and output was detected by photomultipliers. A time constant of about a microsecond was used to smooth both responses. In reality the input signal contains spikes which appear faithfully amplified at the output. In the oscillogram of Fig. 5, the sensitivity of the output detection was reduced 15 db by inserting a grey glass attenuator, and the polarities of both signals are reversed for easier presentation of the data. The figure clearly indicates reduced gain for the later portions of the signal and the resulting pulse sharpening.

The data of Fig. 5 were used to evaluate the intrinsic gain decay curve shown in Fig. 6. Here the ordinate shows the numerical power gain, that is, essentially the amplitude ratio of Fig. 5. The abscissa represents the input energy which was obtained by numerical integration of the lower curve in Fig. 5. The circles show the numerical data points. According to the theory [see (32)], the reduction of gain in this presentation should follow a hyperbola such as shown in Fig. 2. The solid curve in Fig. 6 is a

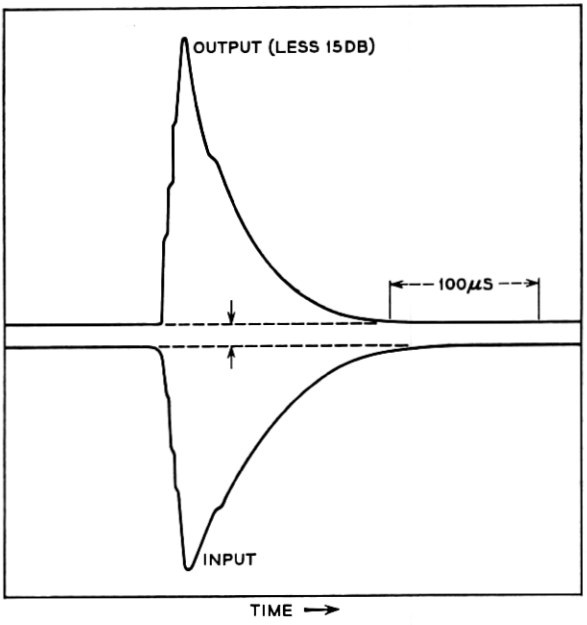

Fig. 5 — Dual-beam oscilloscope record of a pulse sharpening experiment taken with a ruby optical traveling-wave maser by J. E. Geusic.[12] The arrows indicate the time at which half of the energy stored in the amplifier was exhausted, thus reducing the numerical gain by a factor of 2 (or the db gain by 3 db).

hyperbola which was fitted to the data by adjusting two parameters. It should be mentioned that the first and last points of the data are appreciably uncertain because there the absolute magnitude of the signals is rather small. Considering this, the agreement between the data points and the curve is remarkably good. This may be taken as support for the theory. It would be impossible, for example, to fit the data with an exponential law.

Some further details may be read off the curve. The initial gain was 52 (17.2 db). At the time of the signal peak, the gain had already dropped by 1 db to 40.5 (16.1 db). At the point indicated by arrows, the gain is reduced by 3 db to 26 (14.2 db). The energy contained in the output pulse up to that time is equal to the energy originally stored in a 3-db section of the amplifier [(35) applies here, too]. This would be about $\frac{1}{2}$ joule if the output beam filled the entire aperture of the amplifier. Actually, the beam area in this experiment covered one-half of the ruby cross section, so that the output energy, taken from the rise of the pulse to the time marked by the arrows, was about $\frac{1}{4}$ joule. The corresponding average

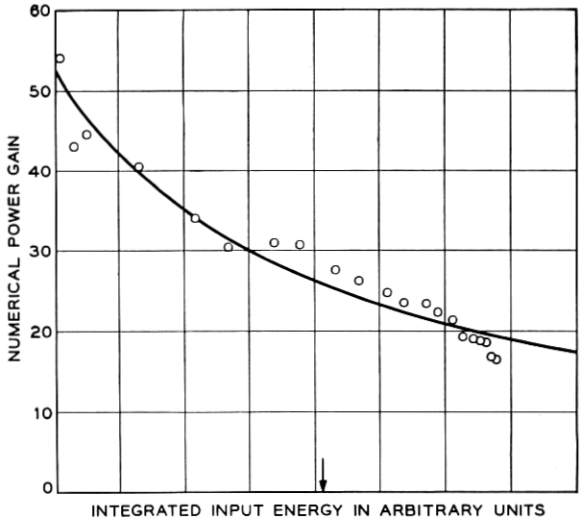

Fig. 6 — Replotting of the data of Fig. 5: numerical power gain is shown vs integrated input energy. Points are data read off Fig. 5 and solid line is hyperbola, predicted by theory, fitted to the data.

pulse power is 5 kilowatts. This power level, incidentally, implies a rather high power per solid angle. The acceptance angle of the amplifier, which was measured to be in agreement with the actual angular spread of the output pulse, is 10^{-3} radians. This comes close to the diffraction-limited beam spread of 10^{-4} radians for a $\frac{1}{4}$-inch diameter ruby amplifier. Application of (33) allows one to evaluate the energy still stored, for example, at the 3-db time. At the output, the stored energy is then reduced to $\frac{1}{2}$ the original value. By comparison, at the input only $\frac{1}{52}$ of the total has been spent. For the latest portions of the signal, the gain has dropped to 20 (13 db), down 4 db from the initial value.

The presentation of the gain data in Fig. 6 shows two other points. Loss of stored energy due to spontaneous transitions is negligible; otherwise the gain would drop faster. This should not occur here, since the pulse is fast compared to the fluorescence decay. The other point concerns the pumping. Fig. 6 shows that the pumping process was completed at the time of the signal pulse, because otherwise an increase in gain with time should be observed.

VI. STEADY-STATE GAIN SATURATION

Under steady-state conditions, the differential equation (5) remains unaltered

$$\frac{dn_t}{dz} = an_t n_z - bn_t \tag{5}$$

and the differential equation (6) becomes the well-known saturation formula

$$n_z = \frac{N_z}{1 + n_t/P_c} \tag{42}$$

where a characteristic saturation power level P_c is defined by

$$P_c = c/a. \tag{43}$$

It is the level which reduces the stored energy to one-half. Another convenient definition is

$$R = aN_z/b \tag{44}$$

the ratio of low-power electronic gain to structure loss. Using (42), (43) and (44), (5) results in the ordinary differential equation

$$(aN_z - b)\frac{dz}{dn_t} = \frac{1}{n_t} + \frac{R}{P_c(R-1) - n_t}. \tag{45}$$

Integration yields

$$\ln \frac{n_t(L)}{n_t(0)} - R \ln \frac{n_t(L) - P_c(R-1)}{n_t(0) - P_c(R-1)} = (aN_z - b)L. \tag{46}$$

This function is an implicit relation between input, $n_t(0)$, and output signal power, $n_t(L)$. If one considers $n_t(L)$ as a function of L, it is a function which has two branches. If

$$n_t(0) < P_c(R-1)$$

a branch results which describes gain. For very small input powers, in particular

$$n_t(0) \ll P_c(R-1) \tag{47}$$

the TWM has simply its low-power gain

$$n_t(L) = n_t(0) \exp (aN_z - b)L. \tag{48}$$

For

$$n_t(0) > P_c(R-1)$$

(46) describes net loss. In particular, for very high input power

$$n_t(0) \gg P_c(R-1) \tag{49}$$

the gain mechanism in the TWM is inactive and the device behaves as an attenuator

$$n_t(L) = n_t(0) \exp(-bL). \tag{50}$$

If the input signal assumes the value

$$n_t(0) = P_c(R - 1) \tag{51}$$

it can be shown that the maser exhibits neither gain nor loss; it is transparent

$$n_t(0) = n_t(L). \tag{52}$$

At this level, the energy stored in the TWM is uniformly distributed

$$n_z(z) = N_z/R. \tag{53}$$

Equation (46) loses its meaning for a TWM without intrinsic loss, $b = 0$. The relation valid in this case may be derived directly from the differential equation or by a limiting process for $R \to \infty$ applied to (46). The result is

$$\ln \frac{n_t(L)}{n_t(0)} + \frac{n_t(L) - n_t(0)}{P_c} = aN_zL. \tag{54}$$

This equation describes an exponential amplification under low signal conditions as before, but an additive amplification process for signal levels large compared to P_c. This means that every section of amplifier having a low-power gain of 4.35 db or a power gain factor of e increases the signal additively by P_c.

For the most interesting range, where input or output power levels are comparable to P_c, (46) has to be applied without approximations. The relation between input, $n_t(0)$, and output power $n_t(L)$ was machine-computed for a number of low-power gain values,

$$G_{\text{db}} = 4.35\ (aN_z - b)L,$$

and gain-to-loss ratios, $R = aN_z/b$. These data are shown in a series of plots in Figs. 7 through 10. Each family of curves applies to masers with the same low-power *net* gain and with the intrinsic loss varied from 3 db to 18 db in 3-db steps. The six families of curves are characterized by low-power net gains from 15 db to 40 db in 5-db steps. Essentially all practical masers are designed for gain in this range. Fig. 7 presents the data as a relation between input and output power, both normalized to the characteristic saturation level, P_c. Fig. 8 shows the apparent gain as a function of input power and Fig. 9 as a function of output power.

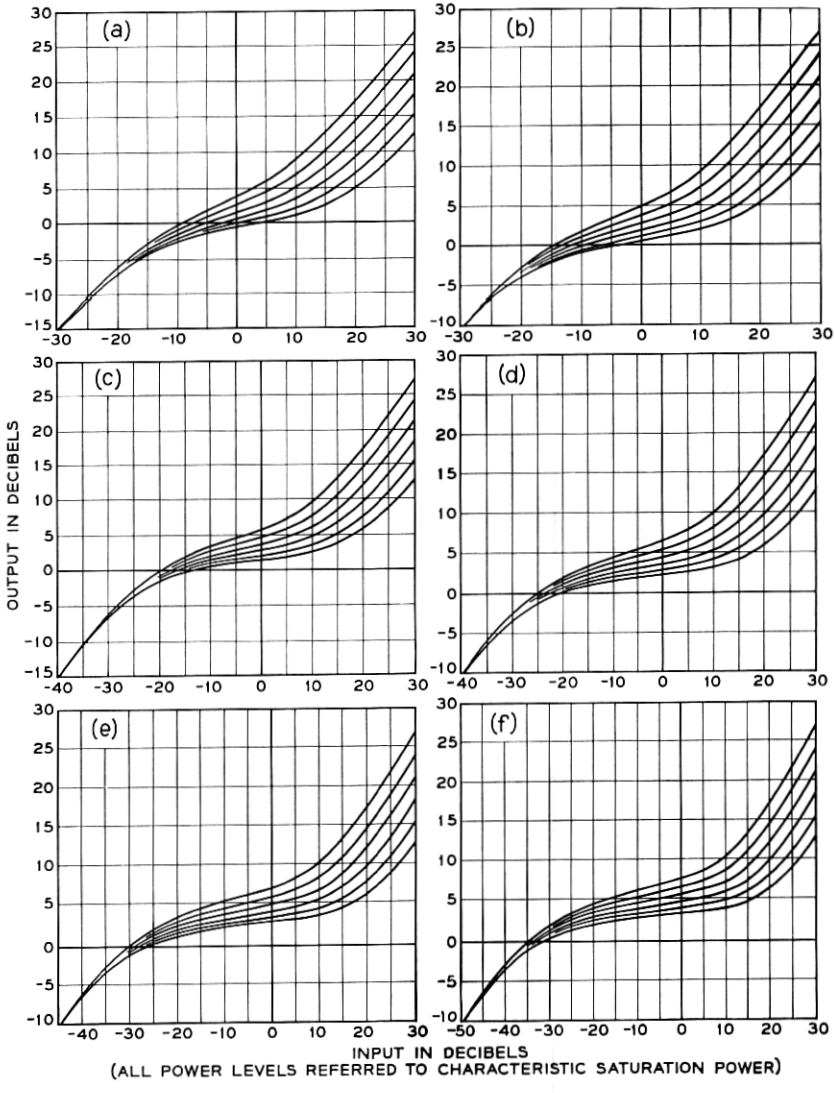

Fig. 7 — Output vs input power for traveling-wave masers having low-level net gain of (a) 15 db, (b) 20 db, (c) 25 db, (d) 30 db, (e) 35 db, and (f) 40 db. Intrinsic loss for each family of curves increases from 3 db to 18 db in steps of 3 db; all power levels are measured relative to characteristic saturation power.

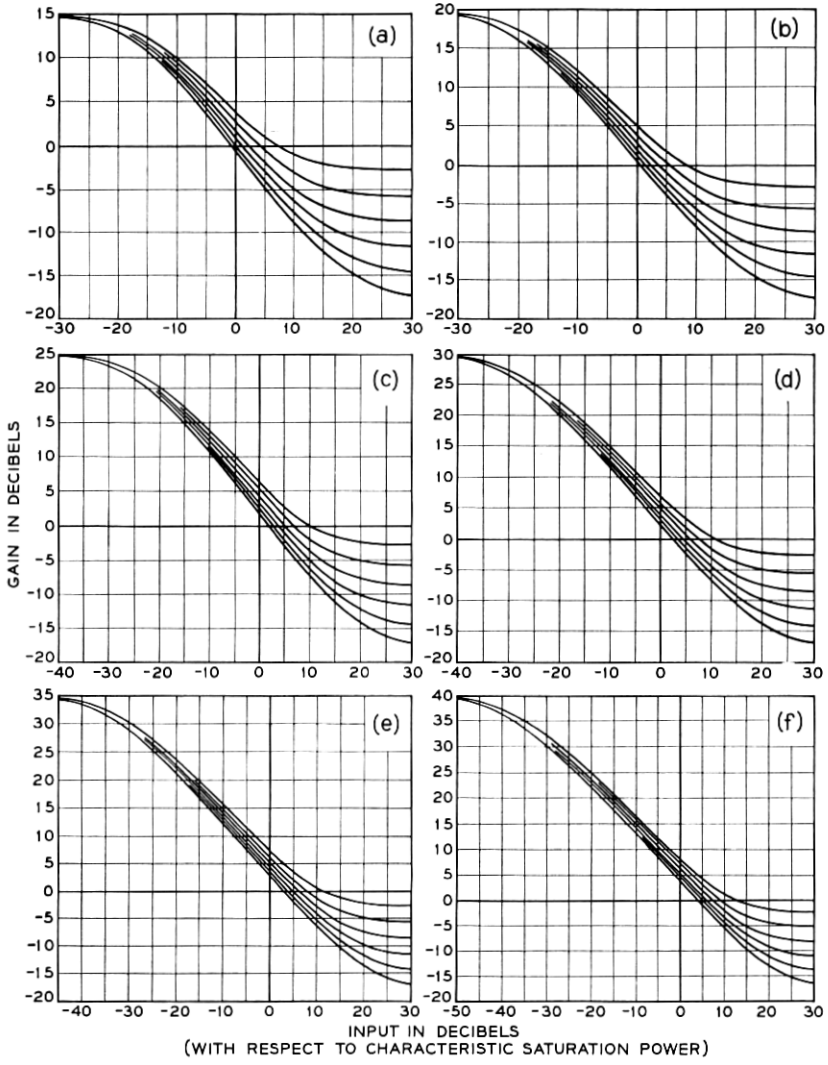

Fig. 8 — Plot of apparent gain vs input power for traveling-wave masers of Fig. 7.

For many applications, the onset of gain saturation in the maser is significant and, depending on the system function, gain compression of ½, 1 or 3 db or even more may be tolerated. The region of beginning gain compression is shown in Fig. 10. It is a plot of apparent gain versus input power as in Fig. 8, although on an expanded scale.

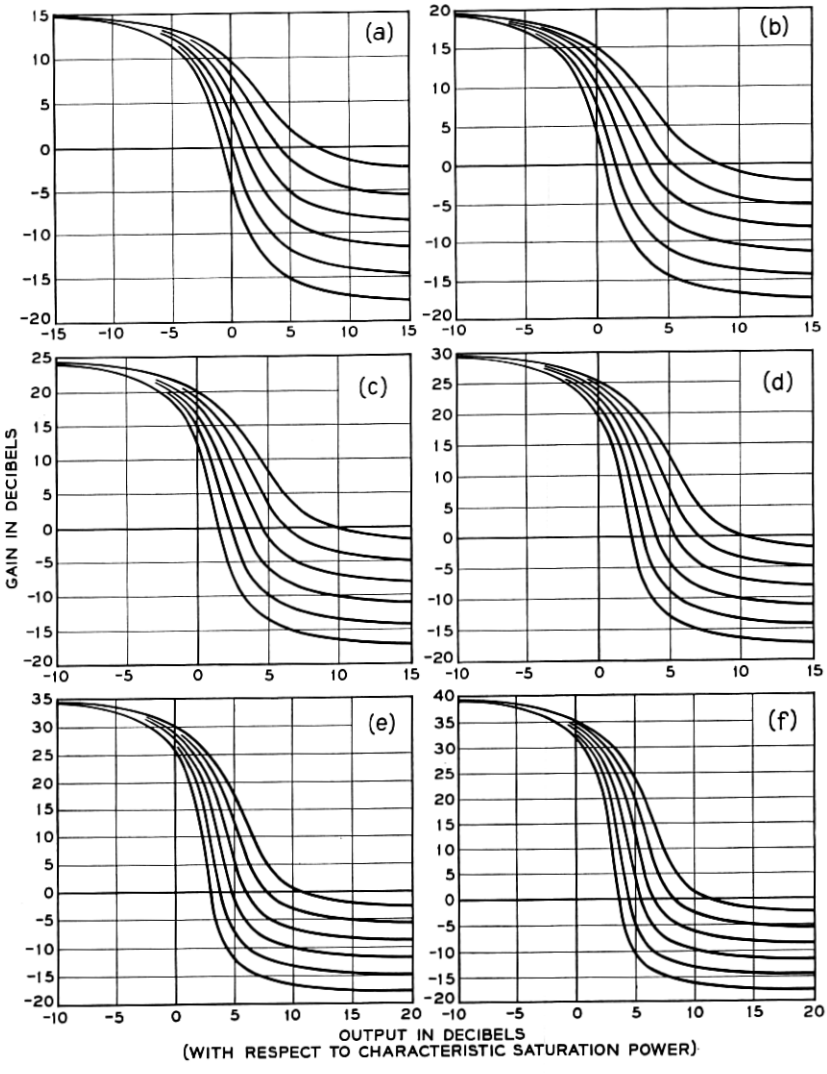

Fig. 9 — Plot of apparent gain vs output power for traveling-wave masers of Fig. 7.

Inspection of Fig. 7, for example, shows that in the range of drastic gain saturation, a TWM can be used for automatic gain control (AGC). Here the average output stays approximately constant for input variations almost as great as the electronic low-power gain. The AGC time constant is nearly, although usually somewhat shorter than, the recovery

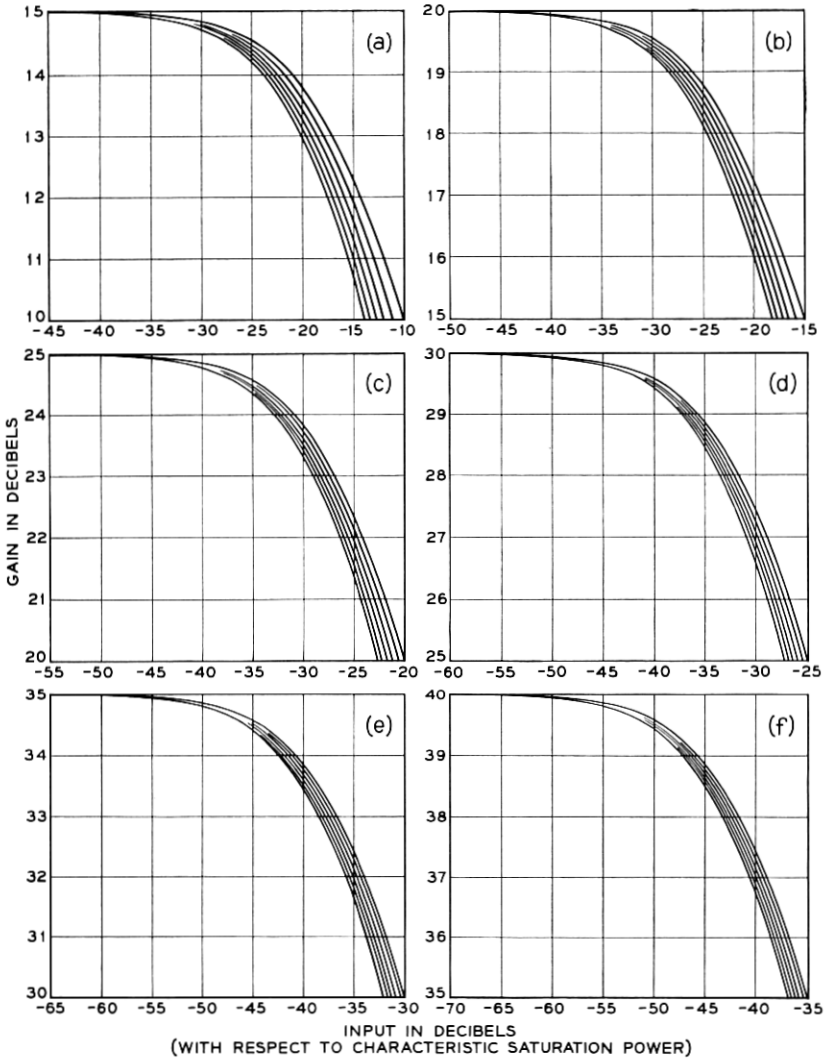

Fig. 10 — Beginning of gain saturation is shown on plot of apparent gain vs input power on an expanded scale for traveling-wave masers of Fig. 7.

time of the TWM, c^{-1}. Masers with high net gain and high intrinsic loss have close to ideal AGC characteristics. It should be pointed out that, over periods of time short compared to c^{-1}, the response of a TWM in an AGC application is still linear, i.e., rapid amplitude variations in the input are strictly reproduced at the output. This distinguishes AGC

action from that of a leveler which clips every power level above a certain minimum without delay. The instantaneous TWM response is more fully discussed in two other papers.[5,6]

For small degrees of gain saturation such as those shown in Fig. 10, it is desirable to have a more manageable approximation of the rigorous, transcendental gain saturation formula (46). The result of a lengthy but straightforward expansion can be given in the form

$$n_i(0)(\text{dbm}) + G(\text{db}) + A = P_c(\text{dbm}) \tag{55}$$

where

$$A = 6.39 + 10 \log_{10} \frac{R}{R-1} - \Delta(\text{db}) - 10 \log_{10} [\Delta(\text{db})]. \tag{56}$$

This formula may be used to solve two typical experimental problems. First, it permits the evaluation of the characteristic saturation power P_c (in units of dbm) from gain saturation measurements. According to (55), P_c is found by the following prescription. Take the input level $n_i(0)$ in dbm at which the gain is reduced by Δ(db), add to it the low-power gain G(db) and a constant A. Typical values of A are given in Table II. Second, the formula and the table (as well as Fig. 10) can be used to study the details of the gain saturation behavior, assuming that P_c is known. For this purpose it may be advantageous to rewrite (55) in terms of the output power

$$\begin{aligned} n_i(L)\ (\text{dbm}) &= n_i(0)\ (\text{dbm}) + G(\text{db}) - \Delta(\text{db}) \\ &= P_c(\text{dbm}) - A - \Delta(\text{db}) \end{aligned} \tag{55'}$$

According to (55′) and the first row of A values, for example, it is apparent that the maser output at 0.5 db gain reduction is about 10 db lower than P_c. Similarly, at 3 db gain reduction the output is roughly 3 db below P_c. One also sees from the table, for example, that gain reduction by 1 db occurs at input levels 3.5 db higher than for a gain reduction of 0.5 db. Similarly, a gain tolerance of −3 db allows 10.3 db greater input signals than a permissible gain compression of 0.5 db. Formula (55) can, of course, also be used in reverse to calculate the

TABLE II — VALUE OF A

	$R = 2$	4	6	8	10
Δ(db) = 0.5	11.9	10.1	9.6	9.4	9.3
1	8.4	6.6	6.1	5.9	5.8
3	1.5	−0.1	−0.7	−0.9	−0.9

maximum permissible input level $n_t(0)$ from a given gain tolerance Δ(db) and the known saturation level P_c.

In the original paper on the microwave TWM,[4] it was suggested that the degree of gain saturation in a maser depends only on average power. Thus the same amount of gain reduction was found with a certain CW power level and with pulses of a 30-db higher peak power applied with a 30-db duty ratio. This feature of maser gain saturation is examined here more closely.

Let t_1 be the duration of signal pulses and t_2 the time after which the pulse repeats. The leading edge of the pulse may be at $t = 0$. Then the energy storage is essentially determined by

$$\frac{\partial n_z}{\partial t} = -an_t n_z \qquad 0 < t < t_1 \tag{57}$$

$$\frac{\partial n_z}{\partial t} = c(N_z - n_z) \qquad t_1 < t < t_2 . \tag{58}$$

In (57), spin recovery is neglected during pulse duration. This leads to a small error for short pulses. The error can be largely compensated for, however, if the recovery in (58) is formally extended over the whole period, $0 < t < t_2$. The solution n_z will be a steady-state solution if it repeats after a time t_2, that is

$$n_z(z,0) = n_z(z,t_2). \tag{59}$$

From (57), (58), (59)

$$n_z(z,0) = \frac{N_z[1 - \exp(-ct_2)]}{1 - \exp\left[-a\int_0^{t_1} n_t\, ds - ct_2\right]}. \tag{60}$$

If the pulses repeat with a fast rate compared to the maser recovery time and if the energy per pulse is not very large, that is, if

$$ct_2 \ll 1 \tag{61}$$

and

$$a\int_0^{t_1} n_t(s)\, ds \ll 1 \tag{62}$$

then (60) can be approximated by

$$n_z(z,0) = \frac{N_z}{1 + \frac{1}{P_c}\frac{1}{t_2}\int_0^{t_1} n_t(s)\, ds}. \tag{63}$$

This equation is identical to (42), the usual saturation formula, except that here the average power takes the place of CW power in (42). Thus all statements made in the equations of this section and in Figs. 7 through 10 are applicable to pulse power, provided the terms used there are interpreted in terms of average power.

In the case of a ruby microwave TWM, the restrictions are not severe. If a safety factor of 10 is included on account of the inequality relations, (61) means that pulse repetition rates should be 100 pps or faster. Since the stored energy in typical microwave masers is between 10^{-6} and 10^{-7} joule, the condition (62) restricts the energy per pulse to about 10^{-8} joule. This may imply 0.1-microsecond pulses of 100 milliwatts or less, or 10-microsecond pulses of 1 milliwatt or less. It is of course possible to operate a TWM under conditions which violate (61) and (62). In that case, the graphs of Figs. 7 through 10 will no longer apply and there will be an appreciable extent of pulse sharpening, as discussed in the earlier sections of this paper.

VII. EXPERIMENTS ON GAIN SATURATION

In this section, some measurements of gain saturation in a microwave traveling-wave maser are reported. The measurements were carried out by F. S. Chen.[3] The maser was developed by P. J. Pantano and W. J. Tabor,[14] and it features the earlier design of a round-finger comb with a single slab of ruby on one side of the comb. The passband extends from 6.2 to 6.8 gc and the highest net gain occurs at 6.25 gc. Signal frequencies of 6.25, 6.35, and 6.45 gc which were used in the measurements are associated with phase shifts between comb fingers of about 20°, 45°, and 75°, respectively.

TWMs of a more advanced design with hobbed square fingers and double-sided ruby loading[15,16] were under development at the time of this study, but they were not available for extended gain saturation measurements. Nevertheless, the general conclusions about gain saturation derived in this section should be equally applicable to those newer masers. The only difference might be the absolute value of the characteristic saturation power.

Four aspects of the TWM gain saturation theory presented in the previous section were studied by the experiments:

(*i*) The theory makes use of a single interaction constant a as defined in (3a). On closer examination this equation suggests, however, that the interaction depends on the local strength of the RF magnetic field, which is a function of the coordinates x,y within the maser material cross sec-

tion A_M. Thus the interaction should be described by a function $a(x,y)$ whose average is equal to the previously used constant a

$$\frac{1}{A_M}\int_{A_M} a(x,y)\,dx\,dy = a. \tag{64}$$

The use of a function $a(x,y)$ implies that there is a varying degree of saturation throughout the cross section of the maser material, i.e. the saturation formula (42) is replaced by

$$n_z(x,y) = \frac{N_z/A_M}{1 + a(x,y)n_l c^{-1}} \tag{65}$$

where

$$\int_{A_M} n_z(x,y)\,dx\,dy = n_z. \tag{66}$$

When introducing (65) into the earlier differential equation (5), it has to be observed that once again the gain interaction $a(x,y)$ varies over the cross section. Thus (5) takes the rigorous form

$$\frac{dn_l}{dz} = \frac{n_l N_z}{A_M}\int_{A_M} \frac{a(x,y)\,dx\,dy}{1 + n_l a(x,y)\,c^{-1}} - bn_l. \tag{67}$$

This equation takes into account the nonuniform exhaustion of stored energy within the maser material cross section, A_M. Parts of the maser material exposed to higher RF fields nearer the comb saturate at a lower signal power level and vice versa. The differential equation (67) predicts a more gradual drop of gain and a slower transition to net attenuation as the input power is increased than the corresponding equation (5) with an averaged value a.

The function $a(x,y)$ was evaluated by F. S. Chen's space harmonic analysis of the comb structure.[17] It consists of a Fourier or space harmonic sum involving combinations of trigonometric and hyperbolic functions. Unfortunately, it is not possible to approximate the result by a simple analytical expression for $a(x,y)$. This is so mathematically because many terms in the sum are of appreciable magnitude, which in turn is due to the physical fact that several of the relevant dimensions are comparable. Thus, while the computed function $a(x,y)$ may be used in machine computations of the gain saturation from (67), this would require a separate set of computations for each comb design and for each phase shift value within the passband (in addition to the number of parameters already entering the computation). Clearly, such a procedure does not appear attractive. Instead, it would be more convenient if it were possible to

interpret the experimental data in terms of the theoretical curves in Figs. 7 to 10, which were computed on the basis of an averaged interaction constant a. In this case one should in principle expect some discrepancy between the theoretical curves and the observed results. The question arises whether this discrepancy, if observable at all, is of practical significance.

(*ii*) The characteristic saturation power, P_c, in (43) is independent of the amount of stored energy in the maser transition. Hence it should be independent of the degree of inversion or the amount of pump power supplied. This feature is obvious from maser theory and would perhaps not deserve experimental verification. For amplifiers other than the maser, however, it would be an unusual property. In conventional voltage amplifiers, for example, the maximum output voltage tends to be proportional to the supply voltage.

(*iii*) The phase shift between comb fingers and the RF magnetic field pattern changes with the signal frequency. This implies a change of $a(x,y)$ and possibly of the average value a with frequency. It is conceivable then that the saturation power P_c varies also with frequency.

(*iv*) The theoretically predicted equivalence of gain saturation by pulse and CW power of the same average value had not been checked before over a large range of power levels.

The experimental results are presented in Figs. 11 to 13. Theoretical

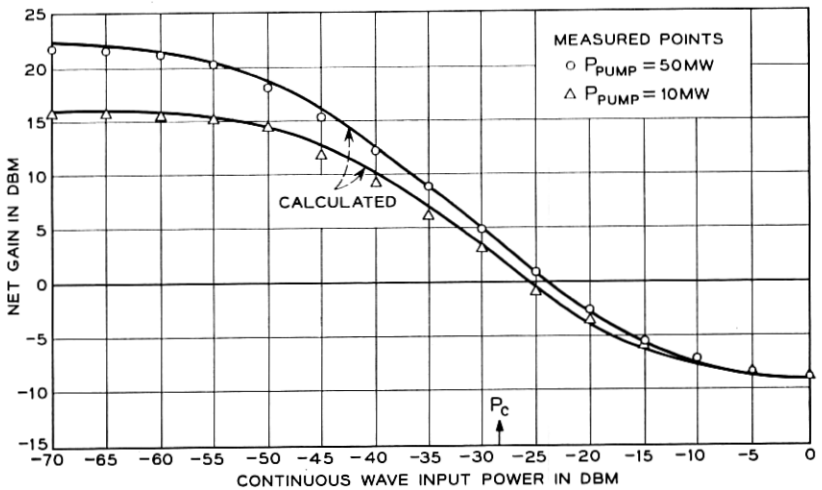

Fig. 11 — Measured and calculated gain saturation under CW conditions. Signal frequency is 6.25 gc and intrinsic circuit loss is 9 db. Fitting of theoretical curves to the data yields a characteristic saturation power level of −28.7 dbm for both curves.

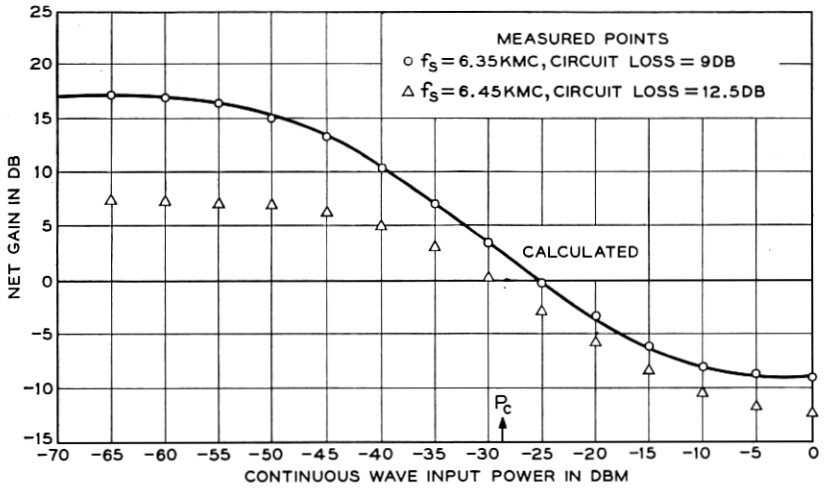

Fig. 12 — Gain saturation under CW conditions at signal frequencies of 6.35 gc (9 db circuit loss) and 6.45 gc (12.5 db circuit loss). The characteristic power level is −28.7 dbm for both curves.

curves taken from Fig. 8 are shown as solid lines, and the experimental data are shown by points and crosses. The theoretical curves were fitted to the data by adjusting the characteristic saturation power, P_c. The figures suggest the following conclusions:

(*i*) The theoretical curves fit the experimental data remarkably well.

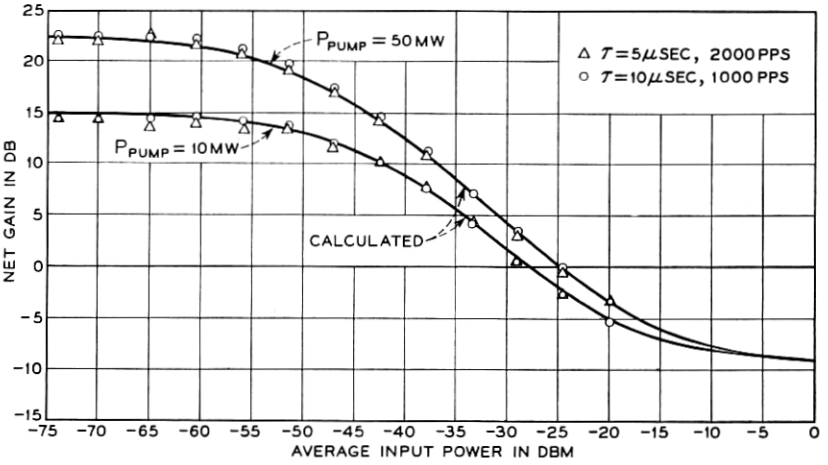

Fig. 13 — Measured net gain under pulse saturation conditions with −20-db duty ratio at signal frequency of 6.25 gc. Data taken with two different pump levels and with two different types of pulses are compared with theoretical curves.

The greatest deviations are ±0.5 db and could in part be caused by experimental errors. There is a consistent tendency of the experimental points, however, to follow a slightly flatter curve than the theoretical one. Nevertheless, gain saturation follows the simplified theory sufficiently well for practical purposes. The discrepancies are ±0.5 db here and could be ±1 db for a maser with 40 db low-power gain. This result eliminates the need for more rigorous computations based on equation (65).

(*ii*) The two curves in Fig. 11, taken with pump power levels of 50 and 10 milliwatts, respectively, are characterized by the same saturation level, P_c, to within better than ±0.25 db. This shows, in agreement with theory, that P_c is independent of the amount of pump power.

(*iii*) The curves in Figs. 11 and 12 result in the same value of P_c, again to better than ±0.25 db for signal frequencies of 6.25, 6.35, and 6.45 gc. In the case of the 6.45-gc data, no compatible theoretical curve was available from Fig. 8, but P_c there was determined from the zero-db conditions (51) and (52). Since all these data were taken only in the lower half of the passband, it is not necessarily justified to assume the same constant P_c in the higher-frequency parts of the passband where the field is even more tightly bound to the comb.

It should be emphasized that a constant P_c across the signal band does not imply that at all frequencies the gain is reduced by 1 db, for example, at the same signal input level. As shown in formula (55), this level depends also on the ratio R and the low-power gain.

(*iv*) The curves of Fig. 13 show the same data with pulse measurements that Fig. 11 shows for CW measurements. Small discrepancies between both figures can be accounted for by the experimental errors inherent in pulse measurements, in particular in an accurate setting of the duty ratio. Taking this into account, the measurements prove over a 50-db range of input power that the degree of gain saturation depends only on average power.

CONCLUSIONS AND ACKNOWLEDGMENTS

The pulse sharpening phenomenon in an optical TWM is, in principle, a means of producing coherent optical pulses of higher peak power and shorter rise time than any other method. The peak power is limited only by the onset of nonlinearities in light transmission, and the rise time is limited only by the linewidth of the optical transition.

Considering the present optical maser technology, however, it would appear difficult to produce pulses of appreciably higher peak power and shorter duration by application of pulse sharpening, compared to those

which are available now by the giant pulse technique. This will have to wait for the development of TWMs which for very short periods of time exhibit very high gain despite the rapid exhaustion of stored energy due to saturation on the intrinsic spontaneous emission. It will also have to wait for the devlopment of more rapid shutter techniques which, for example, may allow a further steepening of the initial rise of a giant pulse so that it may be used subsequently as the driver signal for the TWM pulse sharpening chain. It also should be mentioned that the pulses so produced will show the desirable extremely rapid rise, but a rather slow "hyperbolic" trailing edge. This, however, may be adequate for many purposes, such as high-resolution optical radar.

The analysis of recorded data from a pulse sharpening experiment using a maser of more moderate gain indicates agreement with the theoretical model derived in this paper, in particular with the predicted gain decay.

The gain saturation observed in a microwave TWM distinguishes this device from other amplifiers. In the range of reduced gain, the TWM acts as a slow time constant AGC circuit responding to the signal average power. More rapid signal variations such as modulation of any kind are transmitted and amplified without distortion. At very high signal power, the device is effectively an attenuator of moderate insertion loss. Gain saturation experiments covering power level variations of many orders of magnitude showed that the gain saturation theory derived in this paper is applicable with gratifying accuracy to practical comb structure ruby microwave TWMs. Experiments with pulsed signal power substantiated the suggestion that the degree of gain saturation depends only on the average power.

This work was aided by contributions from many individuals. H. E. D. Scovil predicted the pulse sharpening phenomenon and suggested a study more than four years ago. J. E. Geusic provided the experimental data shown in Fig. 5 on pulse sharpening in his optical TWM. J. A. Morrison conceived the method of solving the pulse sharpening differential equations as reproduced in (11) to (23). W. J. C. Grant programmed the machine plotting of Fig. 3. J. S. Wright programmed the numerical evaluation of (46) and the machine plotting of the data shown in Figs. 7 to 10. F. S. Chen provided the experimental data on gain saturation in a microwave TWM shown in Figs. 11 to 13. He also suggested the derivation of the small gain compression formula (55) and of the average pulse power formula (63). The author gratefully acknowledges these contributions.

Note added in proof. After completion of the manuscript, a paper on

"Pulse Propagation in a Laser Amplifier" by Frantz and Nodvik[18] appeared in print. These authors independently derived some of the results contained in our 1959 report[1] and in certain parts of Sections II, III, and IV of the present paper.

REFERENCES

1. Schulz-DuBois, E. O., Microwave Solid State Devices, U. S. Army Signal Corps Contract DA 36-039 SC-73224, Eleventh Interim Report, November, 1959, p. 14. Available through ASTIA. Unpublished.
2. Wright, J. S., and Schulz-DuBois, E. O., Solid State Maser Research, U. S. Army Signal Corps Contract DA 36-039 SC-85357, Fifth Quarterly Report, September, 1961, p. 33. Available through ASTIA. Unpublished.
3. Chen, F. S., Solid State Maser Research, U. S. Army Signal Corps Contract DA 36-039 SC-85357, Seventh Quarterly Report, March, 1962, p. 11. Available through ASTIA. Unpublished.
4. DeGrasse, R. W., Schulz-DuBois, E. O., and Scovil, H. E. D., The Three-Level Solid State Traveling-Wave Maser, B.S.T.J., **38,** March, 1959, p. 305.
5. Tabor, W. J., Chen, F. S., and Schulz-DuBois, E. O., to be published.
6. Schulz-DuBois, E. O., to be published.
7. Schawlow, A., and Townes, C. H., Infrared and Optical Masers, Phys. Rev., **112,** December, 1958, p. 1940.
8. Maiman, T. H., Stimulated Optical Radiation in Ruby, Nature, **187,** August, 1960, p. 493; Optical Maser Action in Ruby, British Comm. Electron., **7,** September, 1960, p. 674.
9. Collins, R. J., Nelson, D. F., Schawlow, A. L., Bond, W., Garrett, C. G. B., and Kaiser, W., Coherence, Narrowing, Directionality and Relaxation Oscillations in the Light Emission from Ruby, Phys. Rev. Letters, **5,** October, 1960, p. 303.
10. Hellwarth, R. W., *Advances in Quantum Electronics*, ed. J. R. Singer, Columbia University Press, New York, 1961, p. 334; McClung, F. J., and Hellwarth, R. W., Giant Optical Pulsations from Ruby, J. Appl. Phys., **33,** March, 1962, p. 828; Characteristics of Giant Optical Pulsations from Ruby, Proc. IEEE, **51,** January, 1963, p. 46.
11. Geusic, J. E., and Scovil, H. E. D., A Unidirectional Traveling-Wave Optical Maser, B.S.T.J., **41,** July, 1962, p. 1371.
12. Geusic, J. E., and Scovil, H. E. D., Third Quantum Electronics Conference, Paris (1963), to be published.
13. Wagner, W. G., and Lengyel, B. A., Evolution of Giant Pulse in a Laser, J. Appl. Phys., **34,** July, 1963, p. 2040.
14. Pantano, P. J., and Tabor, W. J., Solid-State Maser Research, U. S. Army Signal Corps Contract No. DA 36-039 SC-85357, Fourth Quarterly Report, June 20, 1961, p. 35. Available through ASTIA. Unpublished.
15. Tabor, W. J., and Sibilia, J. T., Masers for the Telstar Satellite Communications Experiment, B.S.T.J., **42,** July, 1963, p. 1863.
16. Hensel, M. L., and Treacy, E. B., private communication.
17. Chen, F. S., Solid State Maser Research, U. S. Army Signal Corps Contract No. DA 36-039 SC-85357, Fourth Quarterly Report, June 20, 1961, p. 27; Fifth Quarterly Report, September 20, 1961, p. 17; Sixth Quarterly Report, September 20, 1961, p. 7; Seventh Quarterly Report, March 20, 1962, p. 1. Available through ASTIA. Unpublished.
18. Frantz, L. M., and Nodvik, J. S., J. Appl. Phys., **34,** Aug., 1963, p. 2346.